Analysis and integration of road projection methods for multiple ground target tracking

S. Gattein
EADS – S & D E
Parc d'Affaires des Portes, BP 613
27106 Val-de-Reuil Cedex, France
stephane.gattein
@eads.com

B. Pannetier
ONERA
92322 CHATILLON, France
benjamin.pannetier
@onera.fr

P. Vannoorenberghe
Laboratoire PSI, FRE 2645 CNRS,
Place Emile Blondel
76821 Mont Saint Aignan, France
Patrick.Vannoorenberghe
@univ-rouen.fr

Abstract *– This paper analyses and evaluates two projection families and describes their integration in a multi target tracker expected to be used in a real world experimentation. The knowledge of the road network allows for more reliable track maintenance and accurate state estimation, compared to standard trackers, when targets are closely spaced and undertake manoeuvres. The methods to be studied are the orthogonal projection, and the probabilistic projection, which are applied to the state estimate. The tracker's estimator uses directional dynamic models corresponding to the roads of interest. The use of competing non-interacting models instead of the interacting multiple model (IMM) method is explained and justified in the context of road targets. The multimodel estimator computes costs, transmitted to an S-dimensional assignment algorithm which determines the best measurement-to-track association. Simulation results show the effectiveness of each projection method on the overall tracking precision, in specific road network and sensor configurations.*

Keywords: Tracking, Ground target, Variable Structure Multiple Model (VSMM) estimator, S-Dimensional Assignment problem.

1 Introduction

This work focuses on a typical multisensor ground surveillance application for which the EADS company is currently developing several data fusion algorithms. Representative tactical scenarios include on-road civil vehicles, convoys of tanks, other off-road capable vehicles, as well as low altitude airborne targets. The ground target tracker that is described here is designed to process consecutive distinct incoming scans from one or more Moving Target Indicator (MTI) radars. Although this algorithm is to be used to produce a tactical ground picture needed by the commanders, this paper concentrates on the tracking of individual targets that are bound to the road network, with the goal of evaluating the effectiveness of the projection functions, and the influence of each of them on the overall tracking precision.

Sec. 2 describes the general architecture of the S-Dimensional Assignment Variable Structure Multiple Model (later called S-D VS-MM) tracker, particularly indicating the interaction of both the estimator and the association modules.

Sec. 3 presents the theoretical basis, and the expected influence of the two internal state projection methods that were implemented in the tracker's estimator.

Sec. 4 details the design of the estimator, that was adapted from [11], and that includes the projection modules.

In Sec. 5, we examine the estimation errors obtained using each of the deterministic and probabilistic projections with a target moving on a single straight road segment (Sec.5.1). These simulations point out the best line of sight versus road orientation configurations where the highest estimator precision is expected. Next in Sec.5.2, the simulation of a standard Kalman filter with different orientations of the measurement error covariance matrix $[R]$, and representative simulation parameters, shows the different geometrical configurations of the filtered state covariance matrix $[P(k+1|k+1)]$ relative to the projection road segment. This allows the interpretation of the estimation errors obtained with the multi target tracker in Sec.5.3 using a real road network.

2 Global tracker architecture

Figure 1 presents the high level structure of the kinematic tracker. The incoming measurements first undergo a systematic alignment which brings them under Cartesian coordinates. Generally, such an alignment module is convenient to convert measurements from dissimilar sensors into a common coordinate system.

The measurements are received in the form of plots belonging to scans, from one or several MTI radars. We assume that the scans are processed in chronological order and never overlap in the time domain, ie: the last measurement of a scan is older than the first measurement of the following scan.

The tracks are managed in two different ways depending on their status: the confirmed tracks are updated using the incoming measurements by the multidimensional

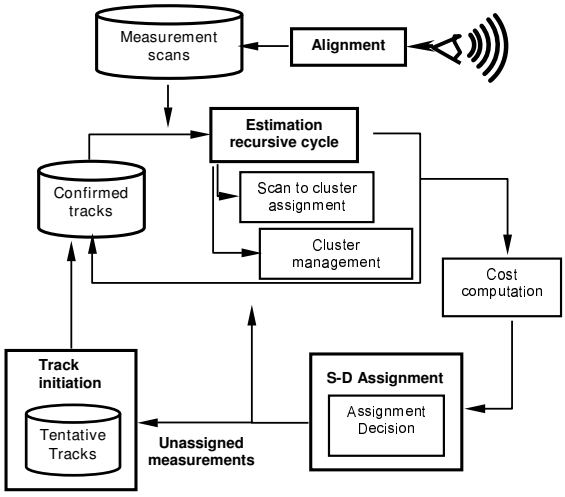

Figure 1: Architecture of the ground target kinematic tracker

assignment, whereas the tentative tracks are updated in a separate function, by those measurements that couldn't be associated to any confirmed track. The confirmed track updating can be seen as a two stage process involving the estimation level, and the assignment level. The estimator computes the track predictions along the roads, determines the feasible measurement-to-track assignments, and updates the track's state on the road network. This updating consists in filtering the predicted state using the assigned measurement before projecting the filtered state on a defined road segment. The estimator operates on each feasible assignment, making no assignment decision. It just computes each assignment cost that informs the assignment module which, in turn, decides which assignment is best, on the multi scan sliding decision window. Finally, when the assignment module has found the best existing association between the list of existing tracks, and the measurements in the S-1 following scans, a hard decision keeps the assignment's decision for the first scan only. After this new track update, the sliding S-1 scan decision window moves to the next scan. A detailed presentation of the 2-D and S-D Assignment operations can be found in reference [11].

3 Projection function principles, definitions, and benefits

The road prior information is used in both the prediction, and projection stages of the above introduced estimator. The projection function can be used only when it is assumed that the target of interest is on-road. In algorithms that can track targets capable of on-road and off-road behaviors, it is necessary to have an opinion on the track's road status in order to correctly apply the projection module. The simulations used in this work assume that all targets are on-road.

Knowing that the MTI radar produces noisy measurements, and that the orientation of its line of sight relative to the roads of interest can vary, the filtered state is always off-road, and the associated covariance matrix doesn't generally reflect the road orientation. The projection algorithms are used to correct the estimated state as well as its associated covariance, according to the segment believed to include the target.

3.1 Measurement under constraint

Some work on projection methods applied to ground target tracking already exists. The deterministic approach was used to orthogonally project the incoming measurement $z_c(k)$ itself [6]. This method computes a projected target observation $z_p(k)$ belonging to the road segment s, whose Euclidean distance to the incoming measurement is minimal. Thus

$$z_p(k) = \arg\min_{z \in s} \left\| z_c(k) - z \right\|_2 \quad (1)$$

A second probabilistic approach is described in [5], and uses the measurement error distribution $[R_c(k)]$ to obtain the most probable target observation $z_{pp}(k)$ belonging to the road network. This position maximizes the *a posteriori* probability $p(z|\ z_c(k), [R_c(k)])$ under the road segment constraint. Thus

$$z_{pp}(k) = \arg\min_{z \in s} \left\| z - z_c(k) \right\|_{[R_c(k)]^{-1}} \quad (2)$$

The analytical expressions for $z_p(k)$, and $z_{pp}(k)$ are given in [1]. However, we preferred to project the target's filtered state rather than the observation itself for several reasons. First an erroneous measurement projection alters future track prediction, and can lead to track loss. Second, the systematic projection of the measurement does not allow to generalize the tracking algorithm to targets that can exit the road network, and whose detections do not necessarily belong to the road. This is why only the internal state projection described below was further considered and implemented.

3.2 Estimated state under road constraint

To comply with the assumption that the target's speed estimate is in the road direction, and that its position estimate belongs to the same road segment *s*, it is possible to process the updated target's state instead of projecting the measurement. Such techniques for projecting the internal state were presented in several target tracking applications [7]-[9], however they only applied the constraint to the target position, except for [8], where the speed vector is projected, but without use of the constrained motion models.

First a *deterministic technique* is described. The estimated state $x(k|k)$ and its covariance matrix $P(k|k)$ can be orthogonally projected on a given road segment s. The resulting state estimate, $\hat{x}_p(k|k)$, whose position is constrained on the segment s, and whose velocity in the direction of s, is the solution of the following equation

$$\hat{x}_p(k|k) = \arg\min_{x \in s} \left\| \hat{x}(k|k) - x \right\|_2 \quad (3)$$

Thus

$$\hat{x}_p(k|k) = P_\perp(s).\left(\hat{x}(k|k) - [x_s, 0, y_s, 0]^t\right) + [x_s, 0, y_s, 0]^t \quad (4)$$

and

$$P_p(k|k) = P_\perp(s) \times P(k|k) \times P^t{}_\perp(s) \quad (5)$$

where $P_\perp(s)$, a 4x4 matrix, is the conventional state orthogonal projection matrix on the road segment *s*. The reader is referred to [9] for the detailed proof of Eqs. (4,5). However this technique does not use the known state covariance *P(k|k)* in the computation of $\hat{x}_p(k|k)$.

Next the *probabilistic state projection* is described. The unconstrained filtered target state *x(k|k)* is the mean value of the posterior state distribution *p(x(k)|Z^k)* [10]. The constrained estimate $\hat{x}_{pp}(k|k)$, resulting from the probabilistic projection, maximizes the probability distribution *p(x(k)|Z^k)*, while also satisfying the road constraints. The probabilistic state projection thus obeys

$$\hat{x}_{pp}(k|k) = \arg\min_{x \in s} \left\| x - \hat{x}(k|k) \right\|^2_{\mathrm{P}(k|k)^{-1}} \quad (6)$$

This probabilistic state projection on road segment *s* satisfies the minimization of the Mahalanobis distance (see [9]). Compared to the projection of the measurement defined by Eq. (2), the state projection uses the additional velocity constraint. For the velocity vector to be parallel to the direction of the road segment *s*, we use the orthogonal condition between the velocity vector and a normal vector to segment *s* called $\vec{n}$. This condition is equivalent to the zero scalar product $\left\langle \vec{\dot{x}}(k) \middle| \vec{n} \right\rangle = 0$.

The minimization problem defined by Eq. (6) can then be written as

$$\hat{x}_{pp}(k|k) = \underset{x, \tilde{D}.x = \begin{bmatrix} -c \\ 0 \end{bmatrix}}{Arg\ \min} \left[\left(x - \hat{x}(k|k)\right)^t .\mathrm{P}(k|k)^{-1} .\left(x - \hat{x}(k|k)\right) \right] \quad (7)$$

where

$$\tilde{D} = \begin{bmatrix} a & 0 & b & 0 \\ 0 & a & 0 & b \end{bmatrix} \quad (8)$$

Using a Lagrangian approach, the analytical expression for constrained *MAP* estimate and its associated covariance matrix are given in [9] and recalled hereunder

$$\hat{x}_{pp}(k|k) = \hat{x}(k|k) - \mathrm{P}(k|k).\tilde{D}^t .\left(\tilde{D}.\mathrm{P}(k|k).\tilde{D}^t\right)^{-1} .\left(\tilde{D}.\hat{x}(k|k) - \begin{bmatrix} -c \\ 0 \end{bmatrix}\right) \quad (9)$$

$$P_{pp}(k|k) = \left([Id] - \mathrm{P}(k|k).\tilde{D}^t .\left(\tilde{D}.\mathrm{P}(k|k).\tilde{D}^t\right)^{-1} .\tilde{D}\right) \times \mathrm{P}(k|k) \times \left([Id] - \mathrm{P}(k|k).\tilde{D}^t .\left(\tilde{D}.\mathrm{P}(k|k).\tilde{D}^t\right)^{-1} .\tilde{D}\right)^t \quad (10)$$

Eqs. (4,5) and Eqs. (9-10) were implemented in the estimator to be described in the next section.

4 The variable structure multi model estimator

The functions handled by the estimation cycle are:
- the management of the feasible dynamic models that each track can follow, based on the set of roads that can be reached by the tracks at the time of the measurement to be assigned. This enables the track's state prediction based on a track context dependant model set.
- the gating of the incoming measurements to determine the feasible measurement-to-track assignments,
- the computation of the cost, which is used as the decision criterion to the assignment function,
- the track's state estimation posterior to the assigned measurement,
- the possible correction of the estimated state, by *projecting* it on the road network when road targets are involved.

The estimation process can be considered as a cycle, since the above steps form a recursive process that can be repeated without any decision on measurement-to-track assignment. Indeed, the estimation and cost evaluation processes are conducted for all feasible assignments in the decision window. These functions will be examined in more detail in the following sections, and the structure of the multi model estimator will be justified.

4.1 Dynamic model management

This section justifies the approach that was implemented to manage the hypotheses on the kinematic behaviour of the targets, and to express their internal states. We especially detail why an IMM approach was not chosen for tracking targets bound to the road network.

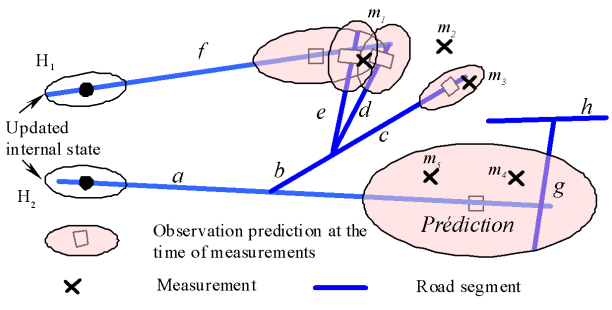

Figure 2: Illustration of road model hypotheses maintenance for a single track

As it is shown in Figure 2, we chose to generate and maintain as *individual and competing* hypotheses all possible *road segment sequences* that the track could follow from its last updated state to the time of the

measurement to which it is predicted. Figure 2 is an example, where, posterior to the assignment of a given measurement, the track could follow two different road segment sequences. Thus the track's internal state is made of hypotheses H_1 and H_2. Figure 2 shows the observation predictions based on this multi model internal state, at the time of the next measurements. In general, the measurements in the scan have slightly different time stamps.

In order to determine all feasible measurement-to-track assignments, predictions must be computed on each track, and on each of their dynamic models, at the time of the candidate measurement. In Figure 2, it can be seen that measurement m_2 can't be assigned to the existing track because no dynamic model is liable to produce such a measurement. Conversely, measurement m_1 can be caused by hypotheses H_1, or H_2. Consequently, the segment sequences *f*, *a-b-e*, and *a-b-d* will compete to explain measurement m_1. For a given measurement-to-track assignment within the decision window, all possible road segment sequences are examined. The following subsections detail the systematic scheme followed inside the estimation cycle.

4.2 Prediction, and determination of the feasible assignments

Posteriorly to the last assignment, all targets are predicted on the basis of each of their dynamic hypotheses. Each such hypothesis assumes the track has followed a given road segment sequence, and thus, is currently on a given road segment. The prediction of each hypothesis is simply done by following the road network. A continuous white noise acceleration model [12] (often called constant velocity model) is used on each generic coordinate *x*. The covariance matrix of the discrete-time process noise *v(k)* along the *x* coordinate axis is,

$$Q(k) = E\left[\vec{v}(k)\vec{v}^{t}(k)\right] = \begin{bmatrix} T^3/3 & T^2/2 \\ T^2/2 & T \end{bmatrix} . q_x \qquad (11)$$

where q_x is the constant process noise intensity expressed in [lenght^2/time^3] whose values are given in Sec.5.2. When a junction is crossed, the hypothesis is split in as many segments leaving the junction. Thus in Figure 2, conditionally to hypothesis H_2, and assuming equal chances of using each segment, the prior probabilities (called P_{prior} in Eq. (12)) of the target to end up on segments *e*, *d* or *c* are equal to 1/2.1/3=1/6. Note that prior knowledge on the compliance of the target type to the road type, or the intent of the target, can cause prior probabilities to be non equal. Note, on Figure 2, that these predictions are used to determine which measurement can be assigned to which track. Thus a measurement that falls inside the validation ellipse of a target for any given model can be assigned to that track. This is the case for measurement m_3. Note also that conditioned on the assignment of measurement m_3, the only possible dynamic sequence is segments *a*, *b*, then *c*.

4.3 Computation of the posterior values

Since no assignment decision is taken by the estimator, posterior values of dynamic model conditioned track state are computed for each measurement that could be assigned. The posterior probabilities of the dynamic road models are updated in the Bayesian framework. Thus, referring to Figure 2, posteriorly to the assignment of measurement m_1, the posterior probability $P\{S_i|\vec{m}_1\}$ that the target follows sequence S_i, $S_i \in \{f, abe, abd\}$ is

$$P\{S_i|\vec{m}_1\} = \frac{P_{prior}(S_i) \times p[\vec{m}_1|S_i]}{\sum_{j\in\{f,abe,abd\}} P_{prior}(S_j) \times p[\vec{m}_1|S_j]} \qquad (12)$$

Note that the sequences such as *abc*, that the track can follow, but whose validation ellipse doesn't include the measurement are neglected in Eq. (12). The track's state update, conditional to the assigned measurement and the road sequence is computed with a standard Kalman filter.

4.4 Projection of the target's state on the road network

Assuming the target is bound to the road network, its filtered state is not necessarily positioned on the road, due to the measurement error. The use of a projection method allows to correct the state estimate and the associated covariance. Consequently, the final track estimated state will always belong to the road. Sec. 5 analyses the impact on tracking performance whether the deterministic or the probabilistic internal state projection is used.

The choice of the segment on which to project the target's state is also an issue. If several road segments are candidates, the segment whose projection is the closest to the initial filtered state must be selected. However, in our implementation, we have chosen to *arbitrarily project the filtered state on the segment that includes the state prediction*. The benefit of this choice is the reduction of the computing load since there is no best projection selection, and no computing of the candidate states and probabilities. Moreover, the dyn*amic hypothesis generation is limited to the prediction stage*. The risk of systematically projecting on the prediction segment is particularly visible when the state predictions come close to a junction. Indeed, the target can actually pass the junction, whereas its estimated state will be projected before the junction. This distance between estimated state and real target position can occasionally lead to higher estimation errors (Figure 11).

4.5 Conclusion on estimator optimality

This section justifies the adaptation of the estimator from [11] to an optimal estimator that is expected to evolve to exploit the interaction between target type data and the individual feasible road segment sequences.

The exhaustive generation and comparison between all feasible road sequences requires more computation than

the IMM, which uses only as many filters as the number of models that can be followed at the time of the measurement of interest [12]. However, it is preferred to the IMM framework for tracking ground targets. Indeed the transition step specific to the IMM aims to update the prior states, associated covariance, and probability for each possible dynamic model, before predicting to the time of the next measurement. This updating is done by mixing different dynamic models followed before transition according to Eq. (13).

$$\hat{x}^{+}{}_{k-1|k-1}(i)=\sum_{l=1}^{M}\pi_{il}\cdot\frac{p_{k-1|k-1}(l)}{p_{k|k-1}(i)}.\hat{x}_{k-1|k-1}(l)$$

$$R^{xx}{}^{+}_{k-1|k-1}(i)=\sum_{l=1}^{M}\pi_{il}\cdot\frac{p_{k-1|k-1}(l)}{p_{k|k-1}(i)}\times \quad (13)$$
$$\left\{R^{xx}_{k-1|k-1}(l)+\left[\hat{x}_{k-1|k-1}(l)-\hat{x}^{+}{}_{k-1|k-1}(i)\right]\left[\hat{x}_{k-1|k-1}(l)-\hat{x}^{+}{}_{k-1|k-1}(i)\right]\right\}$$

where $p_{k|k-1}(i)=\sum_{l=1}^{M}\pi_{il}\cdot p_{k-1|k-1}(l)$, π_{il} are the known transition probabilities from any model *i* to any model *l*, $p_{k-1|k-1}(l)$ is the last updated probability of the target following model l, and "+"denotes the values computed after the IMM transition. Eq. (13) shows the mixing of the internal state $\hat{x}$, and the associated covariance R^{xx} for model *i*. Thus $\hat{x}^{+}{}_{k-1|k-1}(i)$, resulting from mixing, is used as a new prior value for prediction according to dynamic model *i*. However, this modelling is questionable for road targets. Indeed, the mixing of different road models for the purpose of transition does not generally produce another road model. Moreover, model i represents a road that can be reached at the time t_k of the next measurement, and that generally does not exist at the track's current location, at the time of transition t^{+}_{k-1}. Consequently computing an updated state $\hat{x}^{+}{}_{k-1|k-1}(i)$ by mixing, and predicting it according to model i does not reflect the real on-road target trajectory. In addition, the existing algorithm is to be upgraded so the belief on target type can influence the dynamic models (ie: the road segment sequence) that it can follow. This is also a reason why we prefer to maintain all possible segment sequences starting from the beginning of the decision window, instead of combining models at each new measurement assignment.

5 Simulations

5.1 State projections performances

This section describes the influence of the sensor-to-road configuration on the state projection technique precision. For this, we consider a target moving on a single road segment *s* delimited by points *A* and *B* (see Figure 3 to Figure 5 for their coordinates). A simulated MTI sensor is positioned at the origin of the local reference frame, and tracks the target for each Monte Carlo run. The target is detected every 10 seconds with 50 m range and 0.005 rad azimuth standard deviations measurement errors. The target is moving along the road segment *s* at constant velocity (10 m/s). The process noise intensity *q* (see Eq. (11)) is fixed at 0.0018 m^2/sec^3 along the road and $7.5.10^{-4}$ m^2/sec^3 orthogonal to the road.

Let θ be the angle between the sensor's line of sight, and the road direction on which the target is moving. In cases 1, 2, and 3, we have respectively fixed θ to *0*, $\pi/2$, and $\pi/4$ radians. We compare the root mean square estimation error of the determinist, and probabilistic projection techniques in position and velocity on 100 Monte-Carlo runs.

This simulation shows that for the two special cases of road segment orientation (cases 1 and 2), *both* projection techniques give similar estimation errors (Figure 3, and Figure 4). On the opposite, when θ equals π/4 radians (case 3), the difference between estimation errors is clearly visible (Figure 5). More generally, the probabilistic projection technique of the state is more precise or equal to the orthogonal projection technique. Note also that estimation errors are smaller in case 1 were the sensor

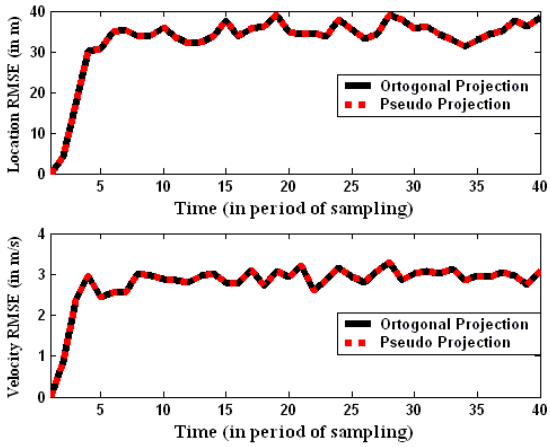

Figure 3. RMSE case 1, A=(45,45)*10^3, B=(40,40)*10^3

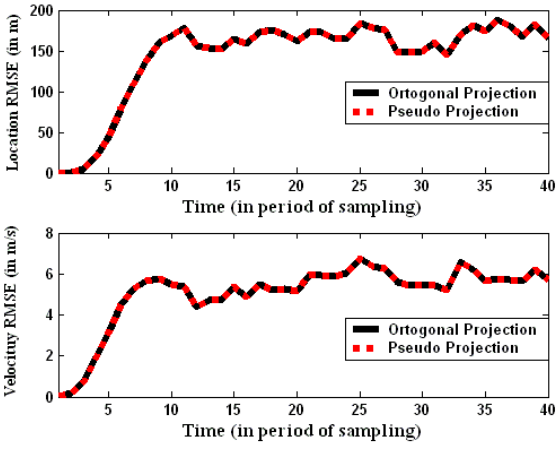

Figure 4 RMSE case 2, A=(47,45)*10^3, B=(45,47)*10^3

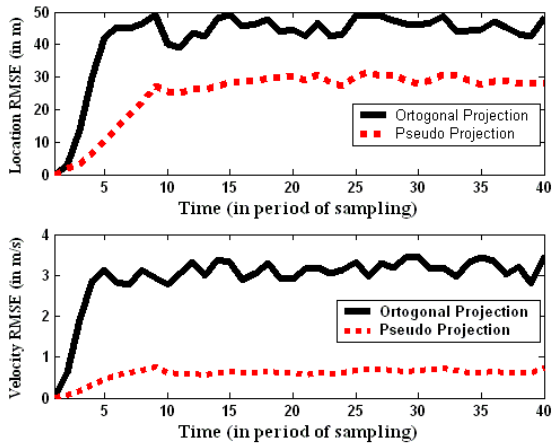

Figure 5. RMSE case, 3 A=(45,45)*10^3, B=(45,42)*10^3

measurement error covariance matrix gives complementary positional information to the predicted state, since its most precise range measurement is in the direction of the road. This can also be seen by comparing Figure 6 and Figure 8.

5.2 Filtering simulations

The Figure 6, Figure 7, and Figure 8 below are results of a standard Kalman filter simulation for a *single target state update*. They respectively correspond to the 99% measurement error ellipses *[R(k+1)]* inclinations of *0*, *π/4*, and *π/2* radians. The goal of this experimentation is to show the covariance matrix orientations of the updated state (*[P(k+1|k+1)]* before projection), that can possibly be encountered with the simulation parameters that will later be used by the S-D Assignment VSMM multi target tracker simulation (Sec. 5.3). Indeed, with a real road network, the sensor-to-road angles can take any value.

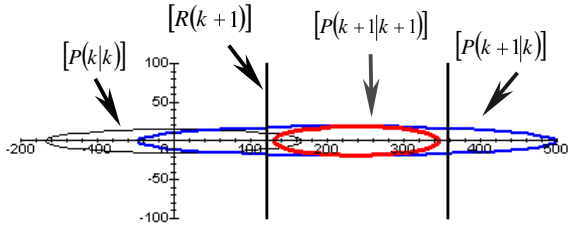

Figure 6: Target state update with *[R(k+1)]* inclined at 0°

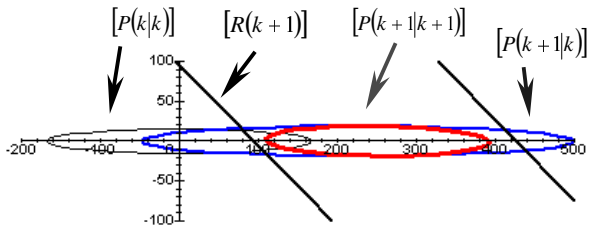

Figure 7: Target state update with [*R(k+1)*] inclined at 45°

The target's initial position is at the center of the reference frame. It moves on a horizontal road segment at constant speed of 15 m/s. The *initial* position and speed estimation error covariance matrices are respectively given by

$$[Ppos(k|k)] = \begin{bmatrix} 3000 & 0 \\ 0 & 25 \end{bmatrix} (m^2) \qquad [Pspeed(k|k)] = \begin{bmatrix} 20 & 0 \\ 0 & 0.01 \end{bmatrix} (m/s)^2 \qquad (14)$$

The longitudinal and orthogonal process noise intensities (see Eq. (11)) are respectively given by q_l =0.5 m^2/sec^3, and q_o =0.01 m^2/sec^3. The time to the associated measurement (t_{k+1}-t_k) is 15 sec. Finally, the positional measurement error covariance matrix expressed in the eigen vector basis is

$$[R_{diag}(k+1)] = \begin{bmatrix} 460000 & 0 \\ 0 & 1511 \end{bmatrix} (m)^2 \qquad (15)$$

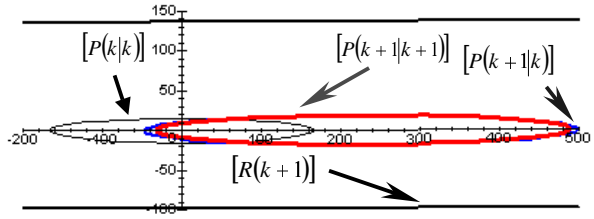

Figure 8: Target state update with [*R(k+1)*] inclined at 90°

The above figures show

- a gain in precision when the sensor's precision is complementary to the road direction (Figure 6), and
- that [*P(k+1|k+1)*] remains oriented in the road direction, in spite of the different possible orientations of [*R(k+1)*].

The nearly constant orientation of [*P(k+1|k+1)*] is due to the strong road directional constraint included in the process noise ($q_o << q_l$). The belief that the target stays on the road segment implies the use of a small value for q_o. Indeed, higher values lead to an important predicted positional imprecision orthogonal to the road. In such cases, the orientation of [*P(k+1|k+1)*] relative to the road could significantly vary.

This section has shown, that for realistic process noise and measurement error values; the orientation of [*P(k+1|k+1)*] stays along the prediction segment. One can thus

anticipate, that the *difference* in estimation error using the deterministic and probabilistic projections will be small, *compared to the estimation errors themselves*.

5.3 S-D VS-MM simulation using a real road network

This section shows the outputs of the multi target tracker on a real road network. The tracking performance is shown in terms of positional estimation error. First the tracking precision difference is evaluated whether a projection algorithm is used or not (Figure 10). In this last case, a two-constant velocity model Fixed Structure Interacting Multiple Model Filter (FS-IMM) [12] is used with $q_f = 0{,}1$ m^2/sec^3, for the non maneuvering model, and $q_F = 0{,}5$ m^2/sec^3, for the maneuvering model. Second, the difference in estimation error is shown whether the deterministic or probabilistic projection is used.

The scenario used in Figure 9 to Figure 11 is based on a real road network in the region of Tarascon, France. The simulated scenario includes 11 road targets moving at approximately 20 m/s; the road segment on which the targets are moving is chosen randomly each time it reaches a junction. A single MTI radar produces one scan every 15 seconds with a 0.9 detection probability. The decision window includes 3 scans, thus the tracker uses a 4-dimensional assignment. The simulated measurement noise *[R]* is that indicated in Eq. (15), inclined at 45°, and represented on Figure 9 (*[R]* not to scale).

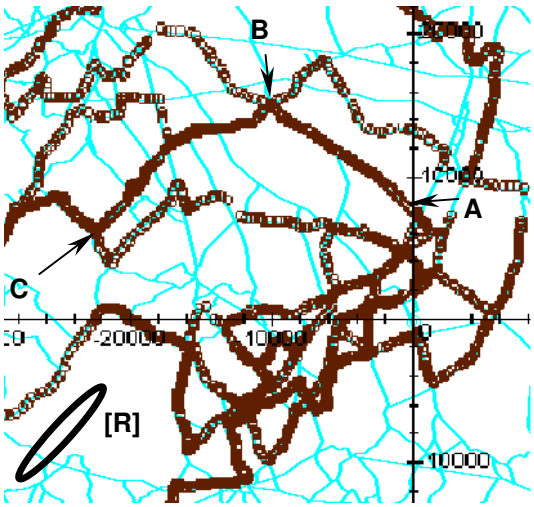

Figure 9: Simulated target trajectories

The target that we chose to focus on in the sequel passes points A, B, and C following an upside-down "V" shaped trajectory on Figure 9.

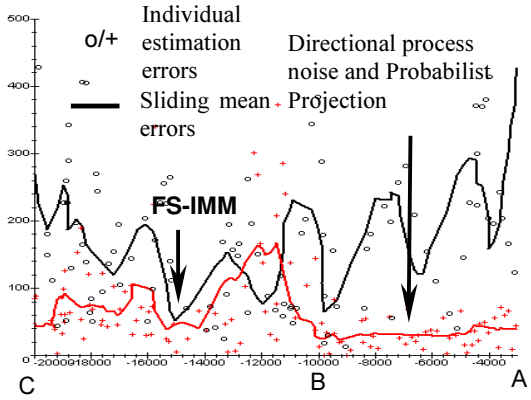

Figure 10: Benefit of modeling the road information (estimation error versus target's abscissa)

Figure 10 shows the obvious gain in estimation precision when the road information is modeled using a directional process noise (values given in Sec. 5.2), and a projection method to adjust the filtered target state. With a Fixed Stucture-IMM, the position errors average about 150m, whereas they average 40m using the road information, when the sensor's line of sight is parallel to the road including the target (road portion from A to B, Figure 9). Figure 11 shows that the position estimation errors for both projection techniques do not differ significantly. This fact can be noticed for other targets whatever the sensor-to-road angle. This result was predicted in Sec. 5.2 and shows that the more the road direction is reflected in the process noise, the less the two projection methods will differ. Moreover, the direction of the road from A to B (Figure 9) varies slightly, further reducing the projection differences. Also a higher precision is clearly visible for both methods for a target x-position >-10000m. This is due to the sensor-to-road configuration similar as for Figure 6.

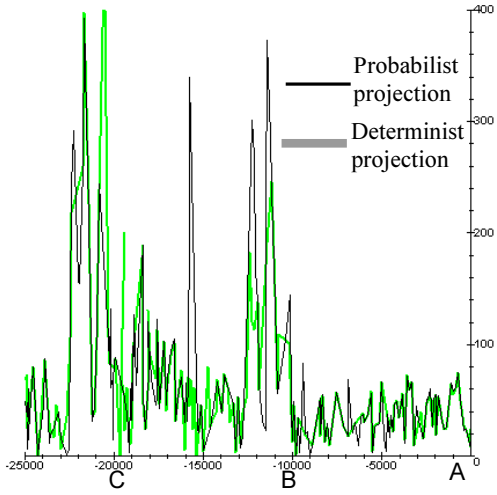

Figure 11: Position estimation error comparison (estimation error versus target's abscissa)

The fluctuations in error estimation values for x<-10000m have two reasons (in addition to the random measurement

errors). First the updated state is systematically projected on the road segment including the state prediction (see Sec. 4.4). This can lead to a higher estimation error when the state prediction is positioned just before a junction. Second, when several dynamic hypotheses are admissible, the synthetic state is computed as a combination of the corresponding projected states. This synthetic state can noticeably differ from the real road target location.

6 Conclusions

An S-D Assignment Variable Structure Multiple Model tracker designed to handle multiple ground targets using a real road network was described. The road information was integrated in the process noise, as well as in the projection methods following state filtering. Both the deterministic and probabilistic projection methods were analyzed, and simulated on a single straight road segment. In this first simple simulation, the projection method proved to produce the most precise estimations. These methods were then integrated in the real road network environment. It was shown that the high-directional road constraints included in the state prediction diminished the possible difference between the two projection methods. Several factors, including constantly changing road direction and systematic state projection on the prediction segment also reduce the difference. Nevertheless, the inclusion of a projection module in the track state updating process was shown to increase the estimation precision dramatically. However, if a projection method is certainly a fundamental step to enhance road target tracking precision, it is no longer sufficient to handle off-road capable targets. Thus the above estimator is currently being generalized to exploit target type data, allowing to recognize the targets' road status, on order to correctly apply road projection methods.

7 References

[1] Pannetier B., Benameur K., Nimier V., Rombaut M., *Ground Target with Road Constraint*, Proc. SPIE, Sensor Fusion, and Target Recognition XIII, Orlando, FL, August 2004.

[2] T. Kirubarajan, Y. Bar-Shalom, K.R. Pattipati, I. Kadar, "Ground target tracking with variable structure IMM estimator", IEEE Trans. On Aerospace and Electronic Systems, Vol. 36, No. 1, pp. 26-46, Jan. 2000.

[3] P.J. Shea, T. Zadra, D. Klamer, E. Frangione and R. Brouillard, "Improved state estimation trough use of roads in ground tracking", *Proc. of SPIE: Signal and Data Processing of Small Targets*, ed. O. E. Drummond, 4048, pp. 321-332, Orlando, FL, Jul. 2000.

[4] B.J. Noe, P.E. Noel Collins, "Variable structure interacting multiple model filter (VS-IMM) for tracking targets with transportation network constraints", *Proc. of SPIE: Signal and Data Processing of Small Targets*, ed. O.E. Drummond, 4048, pp. 247-257, Orlando, FL, Jul. 2000.

[5] J. G. Herrero, J. B. Portas and J. R. C. Corredera, "Use Map Information for tracking targets on Airport Surface", *IEEE Trans. On Aerospace and Electronic Systems*, Vol. 39, No. 2,pp. 675-691, Apr. 2003.

[6] C.C. Ke, J.G. Herrero, J. Llinas, "Comparative analysis of alternative ground target tracking techniques", *Proc. of ISIF*, Paris, Jul. 2000.

[7] D. Nicholson, P.R. Dixon, P.R. Collins, M.I. Smith and M. Bernhardt, "Applying constrained estimators to ground target tracking", *Proc. of SPIE: Signal and Data Processing of Small Targets*, ed. O.E. Drummond, 4728, pp. 247-257, Orlando, FL, Jul. 2002.

[8] D. Simon, T.L. Chia, "Kalman Filtering with state equality constraints*", IEEE Trans. On Aerospace and Electronic Systems*, Vol. 36, No. 1,pp. 26-46, Jan. 2002.

[9] Farina, L. Ferranti, G. Golino, "Constrained tracking filters for A-SMGCS", *Proc. of ISIF*, Cairas, Jul. 2003.

[10] Y. Bar-Shalom, T.E. Fortman, *Tracking and Data Association*, Academic Press, 1988.

[11] Y. Bar-Shalom and W. Dale Blair (editors), *Multitarget-Multisensor Tracking: Applications and Advances*, vol. III, Artech House, 2000, chapters 2 and 6.

[12] Y. Bar-Shalom, X. Rong Li, T. Kirubarajan, *Estimation with Applications to Tracking and Navigation*, Wiley-Interscience, 2001